Supporting Information

High Conversion Propane Dehydrogenation by Photocatalysis under Ambient Conditions

Yucheng Yuan,[+] [a] Yuhan Zhang,[+] [a] Jan Paul Menzel,[b] John Santoro,[a] Madeline Dolack,[a] Hongyan Wang,[a] Victor Batista,[b] Dunwei Wang* [a]

[a] Department of Chemistry, Boston College, Chestnut Hill, MA, 02467, USA

[b] Department of Chemistry, Yale University, New Haven, CT, 06520, USA

[+] These authors contributed equally
Email: dunwei.wang@bc.edu

Experimental section

Materials and reagents

Propane (99.5%), propylene (19.18%, balanced with helium), hydrogen (UHP), and argon (UHP) were purchased from Airgas. All solvents including acetonitrile, acetone, and benzonitrile were purchased from commercial sources and used without further purification unless otherwise stated. Acetonitrile-d3 (CD_3CN, 99 atom% D), sodium tungstate dihydrate ($Na_2WO_4{\cdot}2H_2O$, 99+%), and tetrabutylammonium bromide (TBAB, 99+%) were purchased from Acros organics. Tetraphenylphosphonium bromide (TPPB, 98%) was purchased from Ambeed. N,N',N",N"'-(Tetrafluorodiborato)bis[μ-(2,3-butanedionedioximato)]cobalt(II) dihydrate (COBF, >98%) was purchased from Strem. Chloro(pyridine)bis(dimethylglyoximato)cobalt(III) (COPC) and Nickel(II) bis(trifluoromethanesulfonimide) hydrate ($(Ni(NTf)_2$, 95%) were purchased from Sigma-Aldrich. Dimethylglyoxime ($dmgH_2$, 99+%) and Nickel(II) tetrafluoroborate hexahydrate ($(NiBF_4)_2{\cdot}6H_2O$, 99%) were purchased from Thermo Scientific.

Syntheses of DT catalysts

Sodium decatungstate (NaDT) was prepared via a modified literature procedure.[1] $Na_2WO_4{\cdot}2H_2O$ (22.0 g, 66.7 mmol) was dissolved in distilled water (125 mL), and the solution was heated to 90 °C with stirring. 125 mL of 1 M HCl boiled at 90 °C was added to the solution, and the resulting solution was heated at 90 °C for 40 seconds and then put into an ice bath while stirring. Solid NaCl (90 g) was added to the solution and was stirred at 0 °C for 1 h. Then the precipitate was filtered and washed with DI water (30 mL), ethanol (30 mL), and diethyl ether (30 mL) at 0 °C, and was suspended in hot acetonitrile (2 × 100 mL) while stirring at 90 °C for 30 min. The solution was then centrifuged, and the supernatant was collected in a round-bottomed flask. The solvent was removed by rotary evaporation, and NaDT was collected and dried at 60 °C under vacuum overnight.

Tetrabutylammonium decatungstate (TBADT) was prepared via modification of literature procedure.[2] TBAB (4.8 g, 14.9 mmol) and $Na_2WO_4{\cdot}2H_2O$ (10.0 g, 30.3 mmol) were dissolved in deionized (DI) water (50 mL and 100 mL, separately). The solutions were acidified to pH 2 with concentrated hydrochloric acid solution and then heated to 90 °C. The solutions were mixed at 90 °C, and precipitation was observed immediately, indicating the formation of TBADT. The slurry was stirred for 30 minutes in a 90 °C water bath, then cooled to room temperature, and filtered with a Büchner funnel. The solid phase was washed with DI water and THF (3 × 30 mL) and dried in a vacuum oven at 90 °C overnight. The crude TBADT was further purified by recrystallization in refluxing DCM (1 g : 20 mL) for 2 hours. The mixture was cooled on an ice bath, and then filtered to obtain pure TBADT as a transparent crystal with a light-yellow color.

Tetraphenylphosphonium decatungstate (TPPDT) was prepared via a similar procedure as TBADT. $Na_2WO_4{\cdot}2H_2O$ (1.67 g, 5.06 mmol) and TPPB, (0.76 g, 1.81 mmol) was separately dissolved in DI water (50 mL). The solutions were acidified with concentrated aqueous hydrochloric acid to pH 2 and heated to 90 °C. Then the solutions were mixed at 90 °C, and precipitation was observed immediately, indicating the formation of TPPDT. The slurry was stirred for 30 minutes in a 90 °C water bath, then cooled to room temperature, and filtered with a Büchner funnel. The solid phase was washed with DI water and acetone (3 × 30 mL) and dried in a vacuum oven at 60 °C overnight. The crude TPPDT was further purified by refluxing in acetonitrile (1 g : 20 mL) for 2 hours. The mixture was cooled on an ice bath, and then filtered to obtain pure TPPDT as a white crystal.

To characterize the DT anions in these catalysts, they were dissolved in acetonitrile at a concentration of 10^{-5} M for the UV-vis measurement. The successful syntheses of DT catalysts were confirmed by the characteristic absorption peak at 323 nm in the UV-vis spectra recorded on Agilent Cary 60 UV/VIS Spectrometer.

Measurements of products

The partial pressures of propane and propylene in the gas phase were measured by gas chromatography (GC, SRI Instruments, Multiple Gas Analyzer #5) equipped with a 2-meter HayeSep-D column and a flame ionization detector (FID), while the partial pressure of hydrogen was measured with a

2-meter Molecular Sieve 5Å column and a thermal conductivity detector (TCD). Before measurements, the reactor was charged with Ar to 15 bar as indicated by the gauge on the top of the reactor. Then the reactor was connected to a mass-flow controller linked to the GC instrument. The gases in the reactor were purged at a rate of 15.0 sccm for 10 minutes to clean the GC lines before starting the GC measurement program. All compounds were quantified using external calibration curves generated with calibration standards. A typical chromatogram is shown in Fig. S5. The amounts of propane, propylene and hydrogen in the gas phase were calculated from their partial pressures according to the ideal gas law ($PV = nRT$). The amounts of those gases dissolved in the solution were calculated based on Henry's Law ($P = K_H \chi$), where Henry's law constants K_H of propane and propylene were determined by measuring their solubilities in acetonitrile under different partial pressures (Fig. S6). The K_H of hydrogen was referred to a previous report, which is 5450 bar in MeCN.[3] The yield of propylene was calculated based on the total amount of propane and propylene related by yield% = $n_{propylene}/(n_{propylene} + n_{propane} + n_{byproducts}) \times 100\%$. The yield of hydrogen was calculated via the same way.

Possible liquid byproducts were identified by ^{1}H nuclear magnetic resonance (NMR) spectra. ^{1}H-NMR spectra were recorded on Varian NMR instruments (500 or 600 MHz). Chemical shifts were illustrated in ppm using tetramethylsilane (TMS, 1 v/v% in CD_3CN). Typically, 500 µL of sample solution after catalysis was mixed with 100 µL of CD_3CN. The signal of protons from acetonitrile was significantly higher than those of the products. Thus, a solvent suppression method was used for all ^{1}H-NMR spectra to suppress the acetonitrile signal.

Plots of kinetic files

In addition to the plots of rate-law fitting shown in Figure 3, we also fitted our data using log-log fitting to show the apparent reaction orders intuitively. As presented in the figures below, all reaction orders obtained with log-log fitting are similar to those obtained with rate-law fitting.

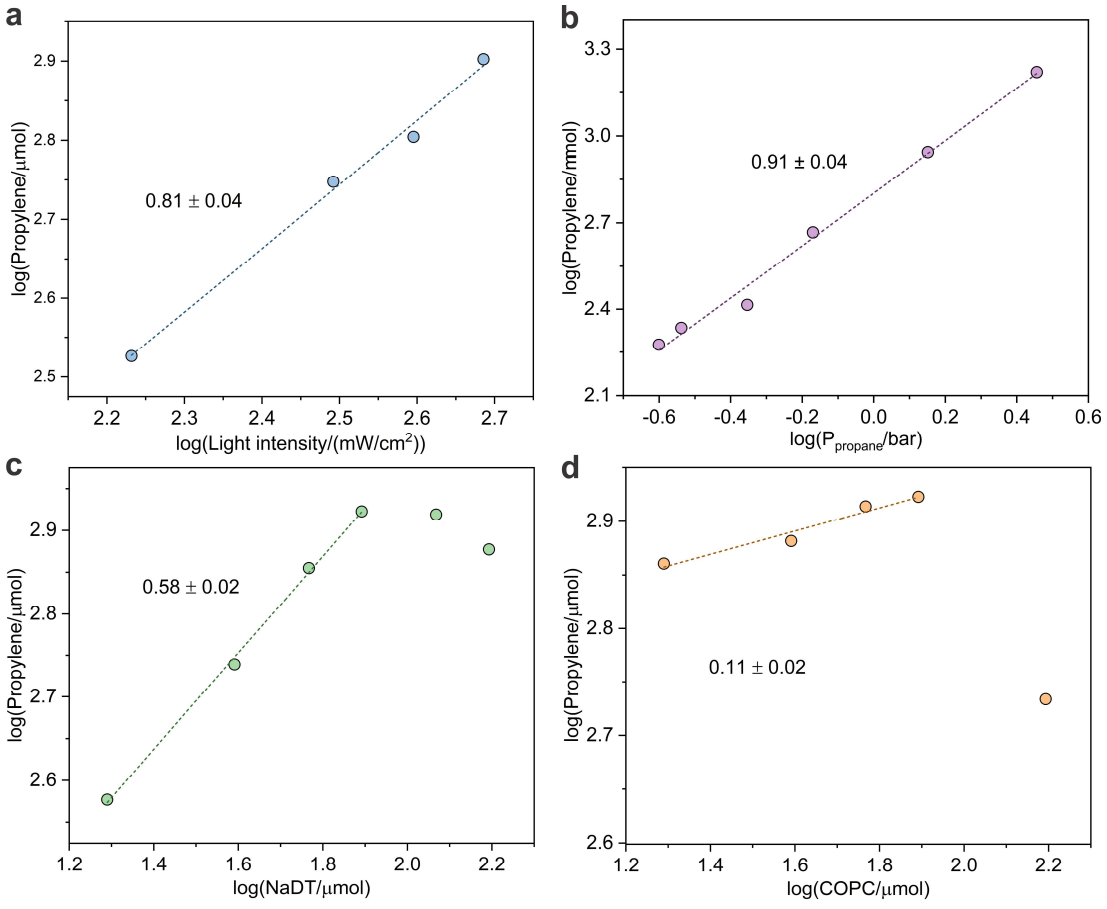

To realize a true initial rate, we derived a function with rate law as follows:

$$-\frac{dP}{dt} = kP^{\alpha}$$

Where P is the pressure of propane and α is the reaction order of propane, therefore,

$$-\frac{dP}{P^{\alpha}} = kdt$$

Then,

$$\int_{P_o}^{P_t}(-\frac{dP}{P^{\alpha}}) = \int_{P_o}^{P_t} kdt$$

And,

$$\frac{{P_0}^{1-\alpha} - {P_t}^{1-\alpha}}{1-\alpha} = kt$$

If the conversion is set as X, then $P_t = P_0\,(1-X)$, thus,

$$\frac{{P_0}^{1-\alpha} - [P_0\,(1-X)]^{1-\alpha}}{1-\alpha} = kt$$

And

$$\frac{{P_0}^{1-\alpha}[1-(1-X)^{1-\alpha}]}{1-\alpha} = kt$$

Thus,

$$P_0 = [\frac{kt(1-\alpha)}{1-(1-X)^{1-\alpha}}]^{\frac{1}{1-\alpha}}$$

Let $\beta = 1 - \alpha$, then

$$P_0 = [\frac{kt\beta}{1-(1-X)^{\beta}}]^{\frac{1}{\beta}}$$

Then, we used curve_fit in python SciPy library to fit β and kt through non-linear least squares, as shown below. Thus, the obtained reaction order was $\alpha = 1 - \beta = 0.87$.

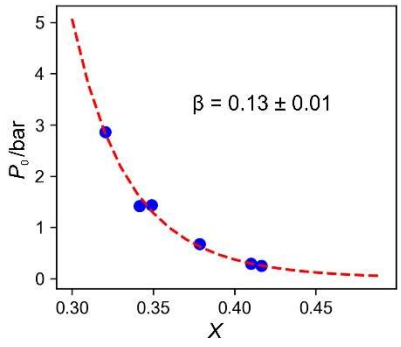

Trapping experiments

To confirm the radical pathway in the reaction system, a trapping experiment was conducted by adding 1 equivalent of TEMPO to the typical reaction system. After 1 h, the reaction mixture was examined using GC-MS (see spectra below). Both TEMPO-trapped isopropyl and propyl radicals were detected, with a ratio of 83:17. Given that the ratio of H atom numbers in secondary positions to those in primary positions is 1:3, the reactivity of C−H bonds in these two positions is approximately 15:1. These trapped species confirmed that in the cooperative catalytic system with NaDT and COPC, the PDH was initialed by the production of propyl radicals.

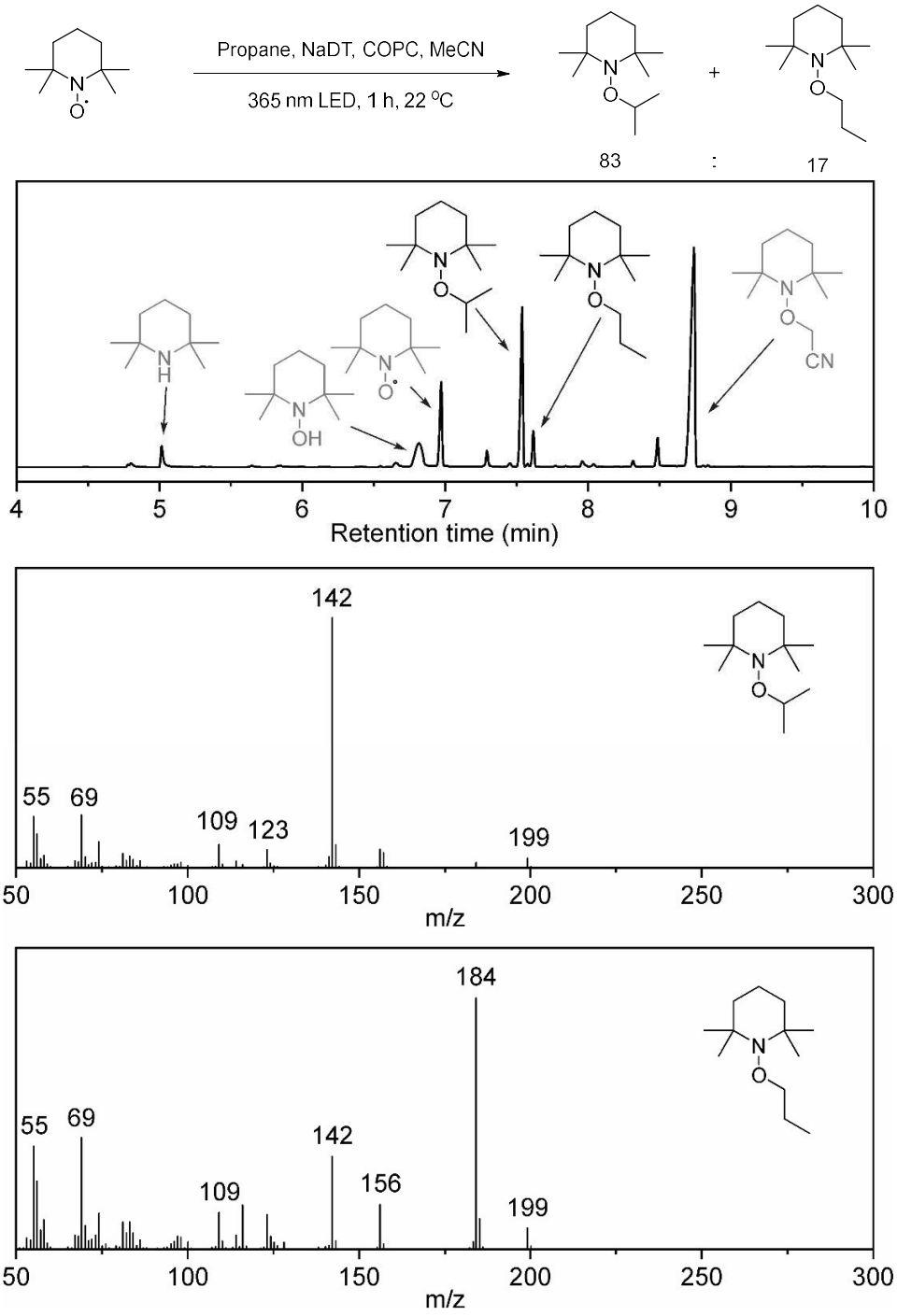

Computational methods

The computational mechanistic study was performed using the Gaussian 16 simulation package.[4] Unrestricted DFT based on the PBE0 functional[5,6] with def2svp basis set[7] was used, including D3 dispersion corrections with Becke-Johnson damping.[8,9] Geometries were optimized in vacuum followed by a frequency calculation, to determine free energy corrections at 298K and 1 atm pressure with the goodvibes program (version 3.1)[10] in the quasi-harmonic approximation.[11] Geometries were reoptimized in implicit acetonitrile, to obtain the energy in solution. The free energy of each intermediate was then obtained by adding the energy in solution to the free energy corrections obtained in vacuum. For the decatungstate in its excited state, the triplet state was used, as it has been shown before that the excited decatungstate quickly relaxes to the lowest triplet state, which is the active reaction partner in the H atom abstraction.[12] Reaction free energy of the excitation of decatungstate was estimated from the difference between ground state and triplet free energies, adding the energy of excitation (365 nm = 3.40 eV). This free energy difference corresponds to the excitation of decatungstate and full relaxation towards the lowest triplet state.

1. Energies in implicit acetonitrile (E_{ACN}), free energy corrections (G_{corr}) obtained from frequency calculations in vacuum and free energy (G_{ACN}) of hydrogen, propane, propyl radical and propylene molecules.

	hydrogen	***propane***	***propyl radical***	***propylene***
E_{ACN} [eV]	**-31.66**	**-3235.67**	**-3217.67**	**-3202.13**
G_{corr} [eV]	**-0.04**	**+2.14**	**+1.65**	**+1.49**
G_{ACN} [eV]	**-31.70**	**-3237.54**	**-3216.02**	**-3200.64**

2. Energies in implicit acetonitrile (E_{ACN}), free energy corrections (G_{corr}) obtained from frequency calculations in vacuum and free energy (G_{ACN}) for decatungstate, active decatungstate and hydrogenated decatungstate.

	decatunsgtate	***decatungstate****	***decatungstate-H***
E_{ACN} [eV]	**-83722.16**	**-83719.60**	**-83737.68**
G_{corr} [eV]	**+1.04**	**+0.97**	**+1.26**
G_{ACN} [eV]	**-83721.12**	**-83718.64**	**-83736.43**

3. Energies in implicit acetonitrile (E_{ACN}), free energy corrections (G_{corr}) obtained from frequency calculations in vacuum and free energy (G_{ACN}) for Co(II), Co(III)-$CH(CH_3)_2$ and Co(III)-H.

	Co(II)	***Co(III)-$CH(CH_3)_2$***	***Co(III)-H***
E_{ACN} [eV]	**-66990.41**	**-70209.51**	**-67006.16**
G_{corr} [eV]	**+7.41**	**+9.98**	**+7.74**
G_{ACN} [eV]	**-66983.00**	**-70199.54**	**-66998.42**

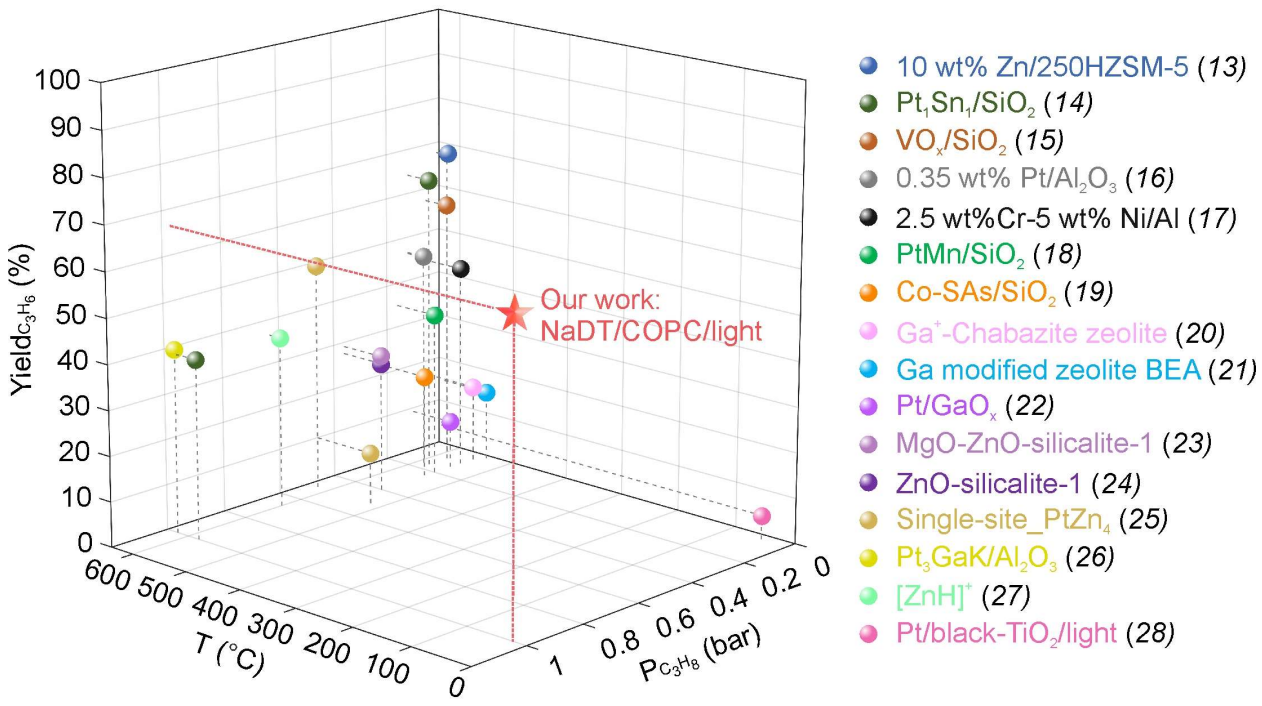

Figure S1. Benchmarking propane dehydrogenation by various catalysts. Our work involves NaDT and COPC as cooperative catalysts, and the process is performed at room temperature and atmospheric pressure, with UV light (λ = 365 nm; Power: 485 mW/cm^2) as an energy input. $Yield_{C3H6}$ = $Conversion_{C3H8}$ × $Selectivity_{C3H6}$. Note: The reference numbers in the parentheses correspond to references in the main text.

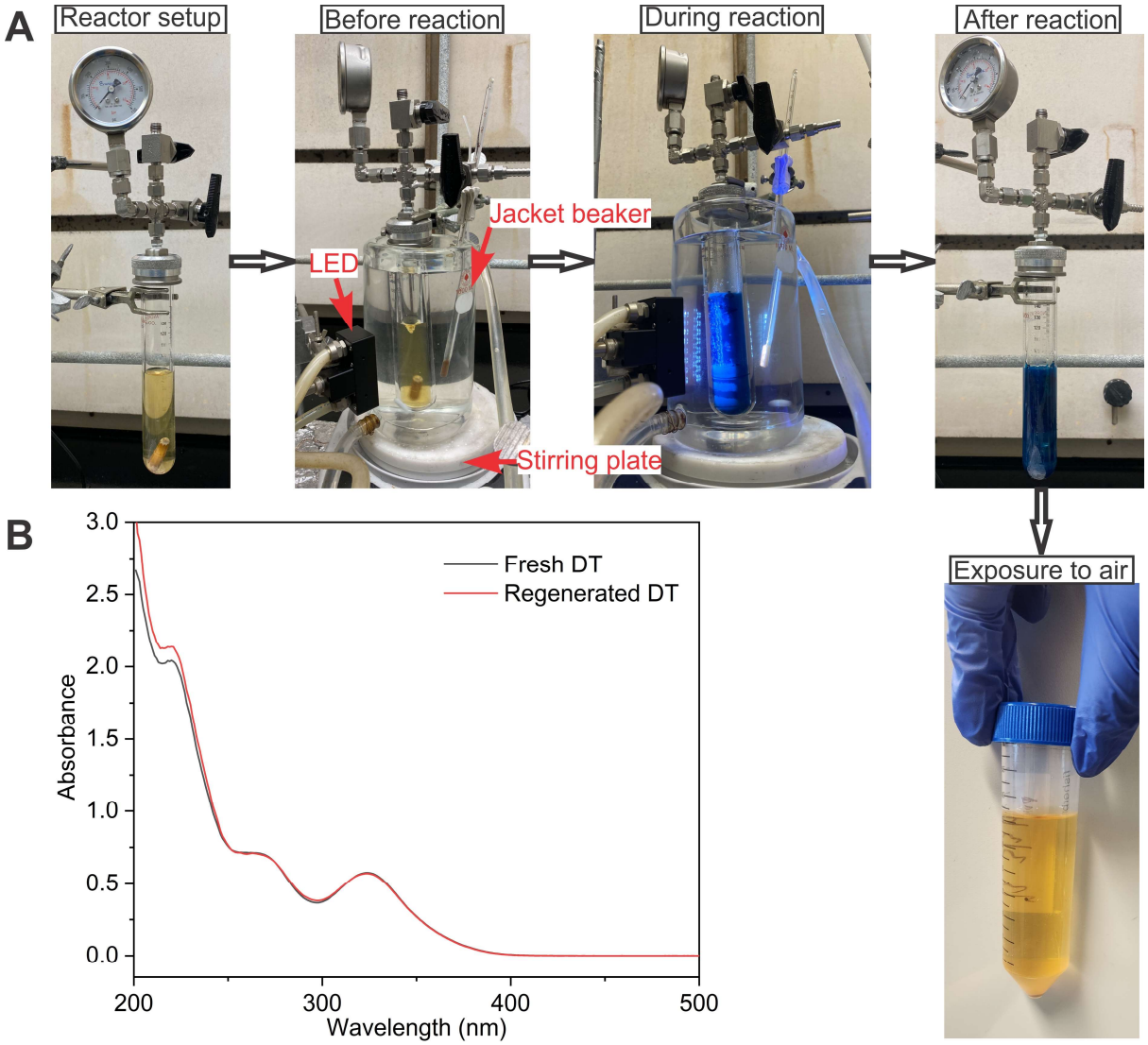

Figure S2. (A) Pictures of experimental setup for PDH reactions. The characteristic blue color corresponds to reduced W centers, including some of the following species: singlet excited state of decatungstate (*$[W_{10}O_{32}]^{4-}$), reactive state of decatungstate (wO), $[W_{10}O_{32}]^{5-}$, and $[W_{10}O_{32}]^{6-}$.[13] These species can be re-oxidized with exposure to air. (B) Comparison of UV-Vis spectra of fresh and regenerated DT species. The regenerated DT species retained their structural integrity, as indicated by their unchanged UV-Vis spectrum. The recyclability test also confirmed that their catalytic ability was similar to that of fresh ones after regeneration.

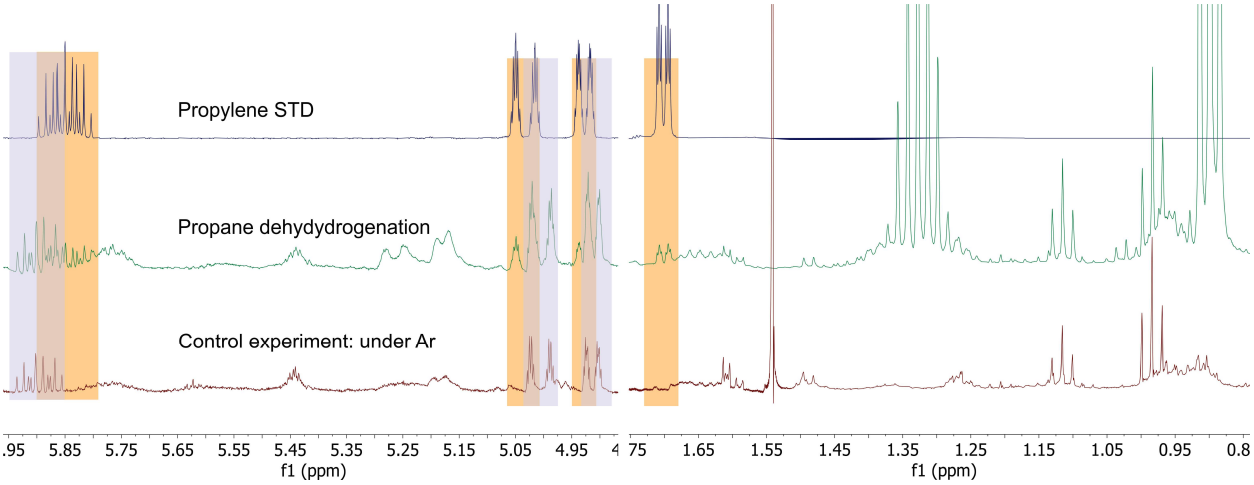

Figure S3. ^{1}H NMR spectra obtained using TBADT/COPC system. The control experiment under Ar atmosphere indicated but-1-ene was produced from TBA cations.

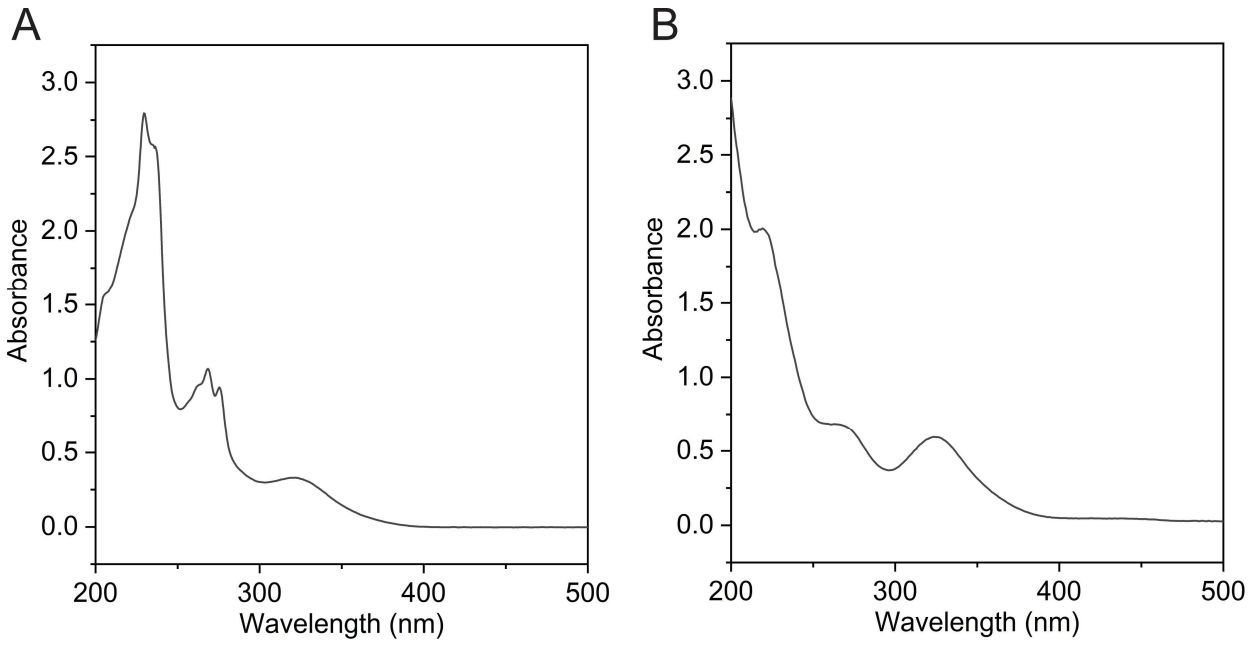

Figure S4. UV-vis spectra of TPPDT (A) and NaDT (B) in acetonitrile.

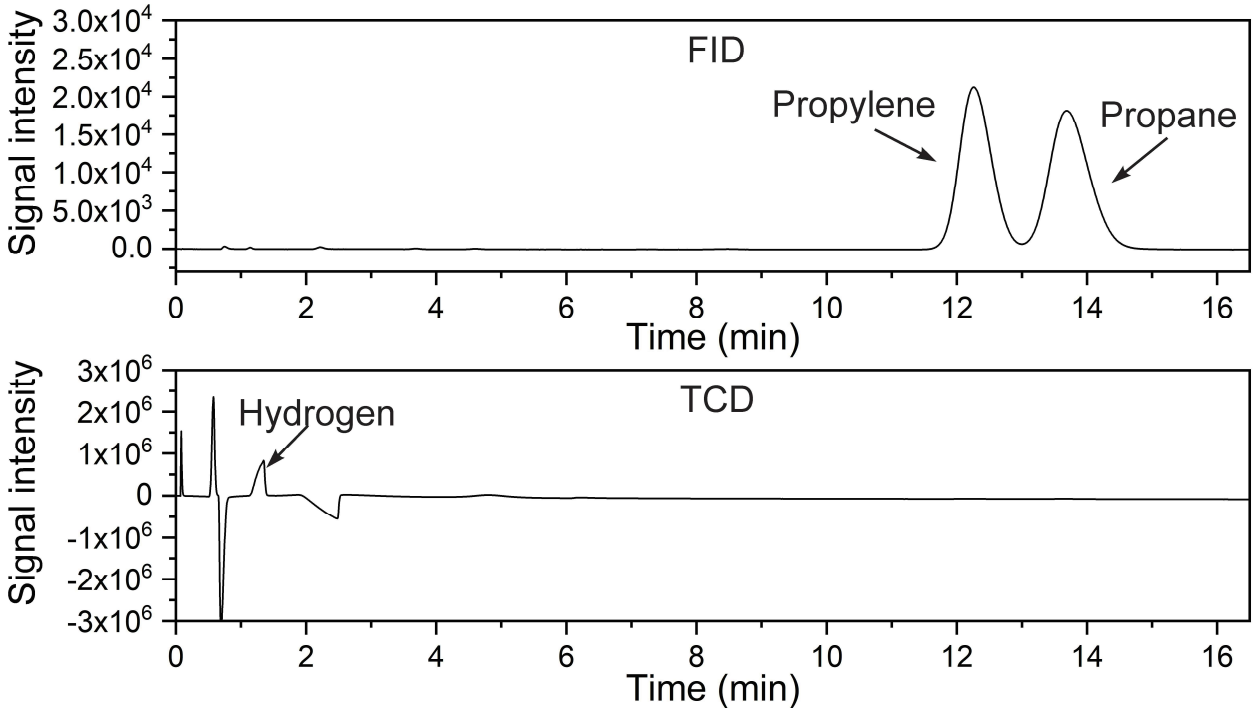

Figure S5. Typical GC chromatogram obtained after a PDH reaction. Reaction conditions: 1 atm of propane was introduced into a vacuumed reactor (85 mL) containing 3 mol% of NaDT, 3 mol% of COPC, and 9 mol% of $dmgH_2$ dissolved in 40 mL of acetonitrile. The resulting mixture underwent irradiation with 485 mW/cm^2 of 365 LED light for 20 h at 22 °C.

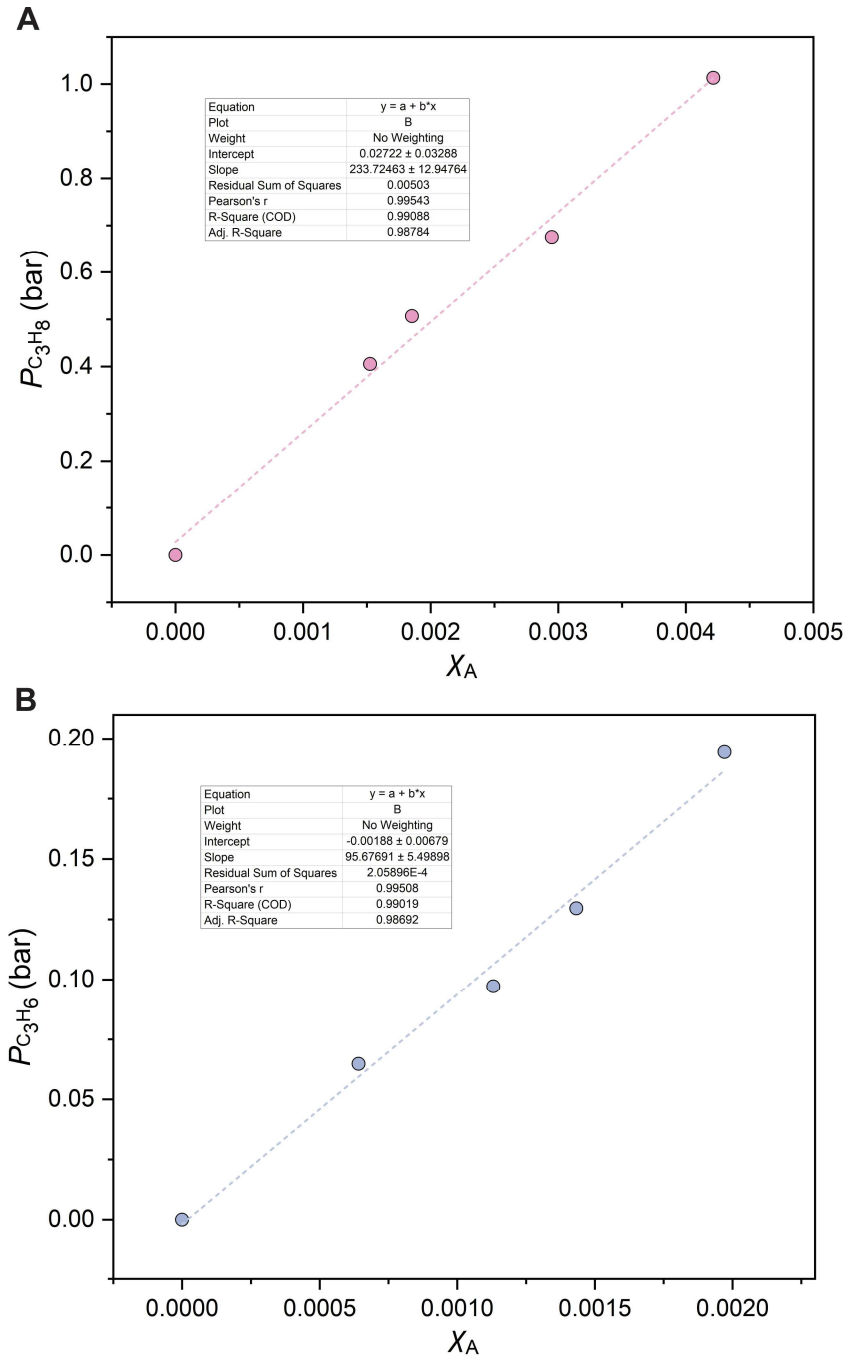

Figure S6. Measurements of K_H of propane and propylene in acetonitrile. χ_A represents the mole fraction of solute gas in the liquid phase. The K_H of propane and propylene are 233 bar and 96 bar, respectively.

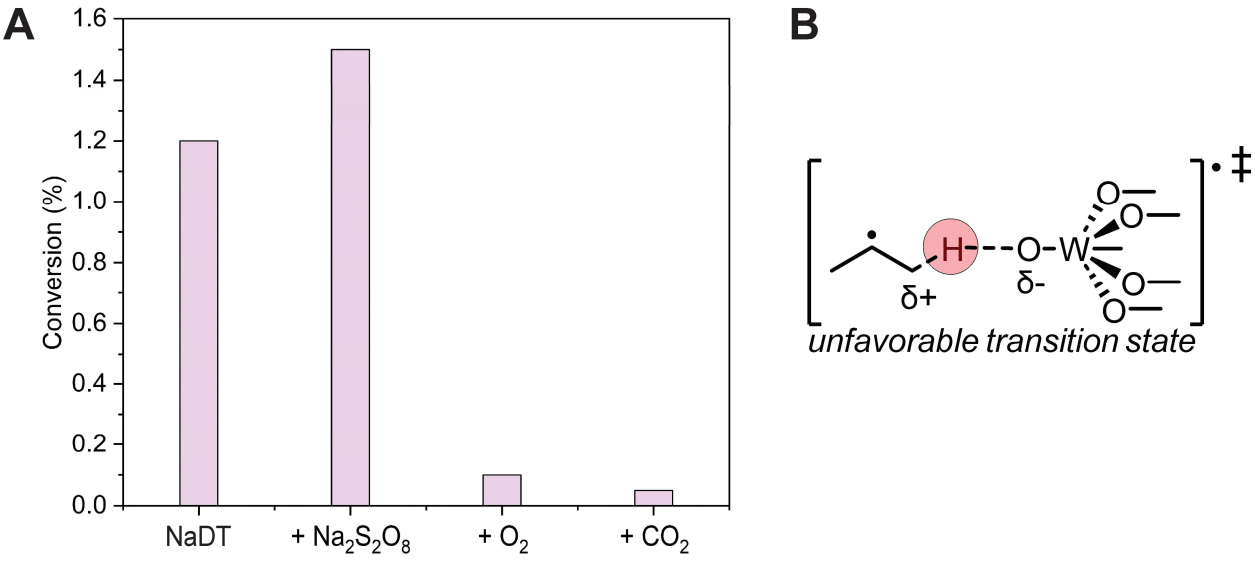

Figure S7. (A) Oxidative PDH with NaDT and different oxidants. (B) A possible reason for the poor performance with the oxidative PDH pathway.

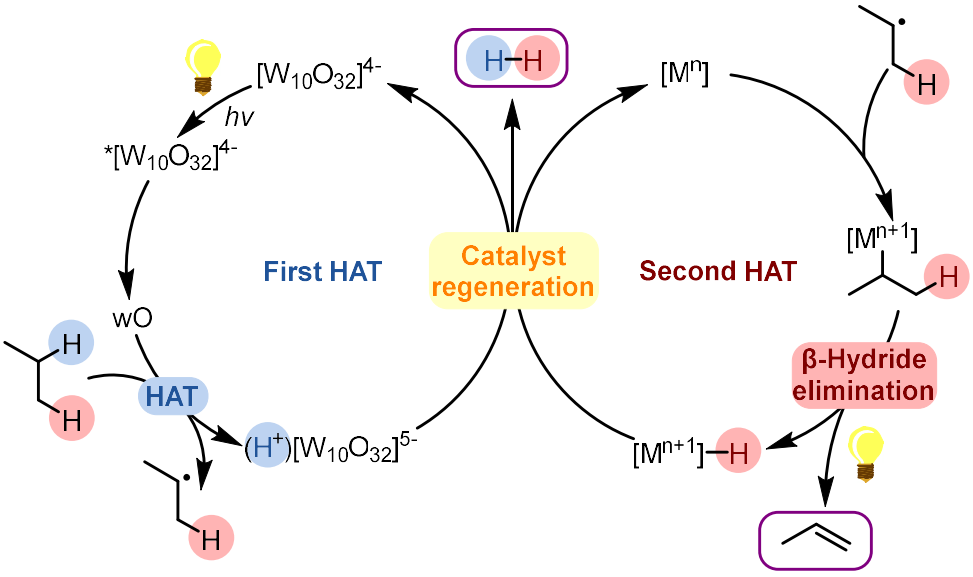

Figure S8. Proposed mechanism of cooperative dehydrogenation pathway.

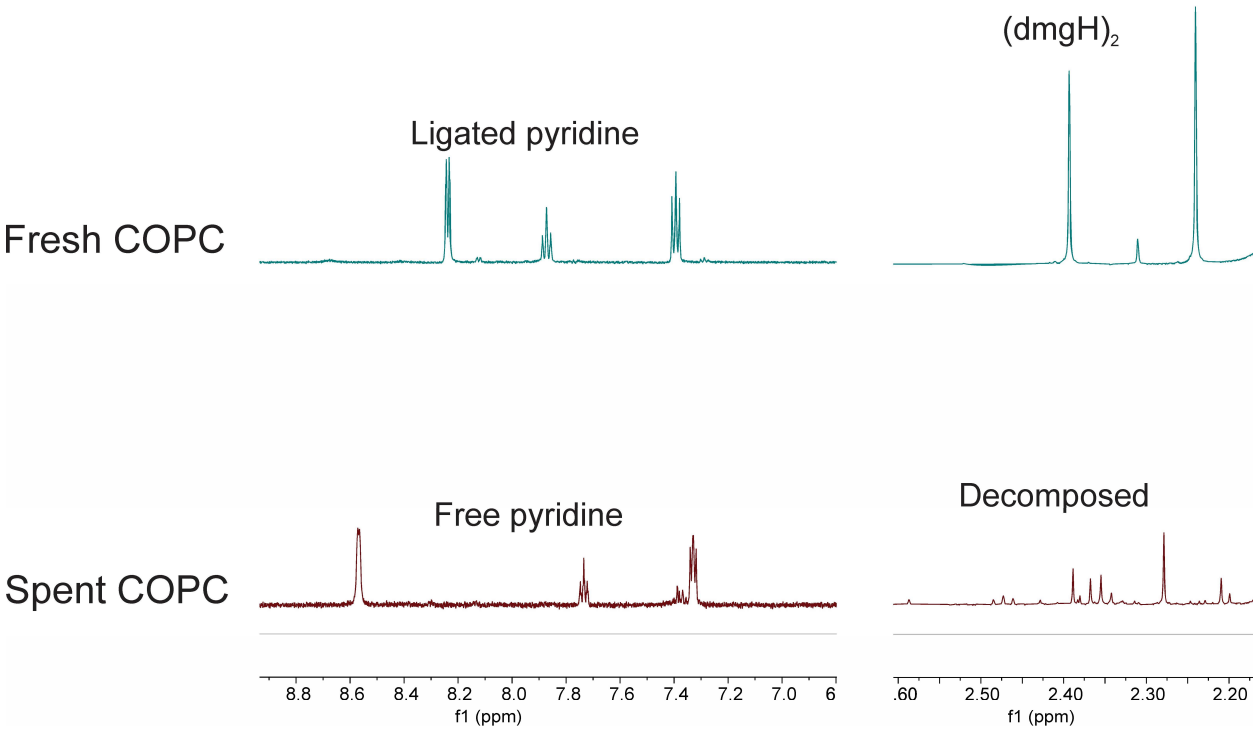

Figure S9. ^{1}H NMR spectra of fresh and spent COPC in CD_3CN.

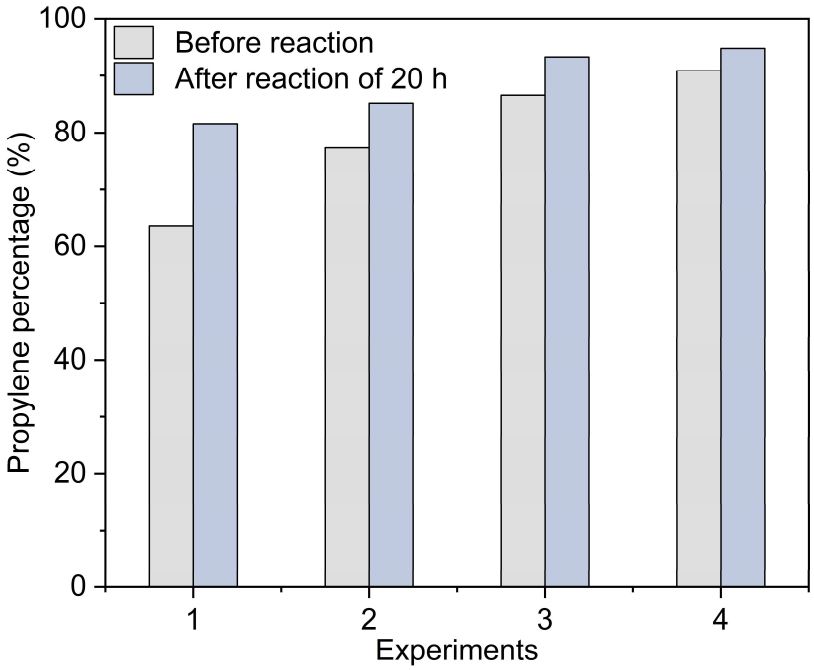

Figure S10. Reactions of pre-mixed gas mixture to understand the conversion limit of PDH under the cooperative system.

Table S1. Summary of the catalytic data of PDH catalysts in **Figure S1**.

#	Catalyst	Reactor	T (°C)	P (atm) (balanced gas)	C (%)	S (%)	Y (%)	STY ($mmol_{C3H6}$ g_{cat}^{-1} h^{-1})	Ref.
1	DT/COPC/light	Batch	22	1.00 (N/A)	68.9	99	68.2	2.63	This work
2	Pt/black-TiO_2/light	Batch	43	0.033 (N/A)	6.0	89	5.3	0.64	28
3	10 wt% Zn/250HZSM-5	Flow	600	0.05 (N_2)	74.0	93	68.8	2.29	13
4	Pt_1Sn_1/SiO_2	Flow	580	0.16 (He)	66.0	99	65.3	69.80	14
5	Pt_1Sn_1/SiO_2	Flow	580	1.00 (N/A)	40.0	99	39.6	42.30	14
6	VO_x/SiO_2	Flow	580	0.09 (Ar)	65.0	90	58.5	2.52	15
7	0.35 wt% $PtSn/Al_2O_3$	Flow	590	0.16 (0.20 H_2/0.64 N_2)	48.7	98	47.7	101.90	16
8	2.5 wt% Cr-5 wt% Ni/Al	Flow	550	0.10 (Ar)	47.0	96	45.1	3.95	17
9	$PtMn/SiO_2$	Flow	550	0.20 (Ar)	39.9	96	38.3	581.27	18
10	Co-SAs/SiO_2	Flow	550	0.24 (N_2)	24.0	95	22.8	15.03	19
11	Ga^+-Chabazite zeolite	Flow	550	0.05 (N_2)	17.7	96	17.0	9.73	20
12	Ga modified zeolite BEA	Flow	540	0.02 (He)	19.0	82	15.6	7.92	21
13	$0.03Pt/3GaO_x/Al_2O_3$	Flow	600	0.14 (0.14 H_2/0.72 N_2)	12.0	95	11.4	96.90	22
14	MgO-ZnO-silicalite-1	Flow	550	0.40 (N_2)	32.0	89	28.5	13.80	23
15	ZnO-silicalite-1	Flow	550	0.40 (0.20 H_2/0.40 N_2)	30.0	96	28.8	120.00	24
16	Single site_$PtZn_4$	Flow	520	0.50 (0.50 H_2)	12.0	95	11.4	10.36	25
17	Single site_$PtZn_4$	Flow	620	0.50 (0.50 H_2)	53.0	95	50.4	45.82	25
18	Pt_3GaK/Al_2O_3	Flow	620	1.00 (N/A)	41.9	97	40.6	19.94	26
19	$[ZnH]^+$	Flow	600	0.67 (0.33 H_2)	43.0	88	37.8	40.38	27

Note: For the STY calculation, the highest yields in each report were used, and the stability of the catalysts were not considered. In this work, the STY was calculated based on a 3-hour reaction with a propane pressure of 4.23 bar, considering the reduction in propane concentration along with the reaction in the batch reactor. The reference numbers correspond to references in the main text.

Table S2. Summary of the catalytic data of photocatalytic PDH and EDH.

#	Rection	Catalyst	Reactor	T (°C)	P (atm) (balanced gas)	C (%)	S (%)	Y (%)	STY ($mmol_{product}$ g_{cat}^{-1} h^{-1})	Ref.
1	PDH	DT/COPC	Batch	22	1.00 (N/A)	68.9	99	68.2	2.63	This work
2	PDH	Pt/black-TiO_2	Batch	43	0.03 (N/A)	6.00	89	5.34	0.64	28[a]
3	PDH	V/TiO_2	Flow	500	0.05 (0.95 N_2)	0.418	98	0.412	0.34	14
4	EDH	DT/COPC	Batch	22	1.00 (N/A)	26.8	99	26.5	1.0	This work
5	EDH	$LaMn_{1-x}Cu_xO_3$	Flow	452	0.09 (Ar)	4.90	91	4.46	1.1	61[a]
6	EDH	Pd-ZnO	Batch	50	1.00 (N/A)	0.177	95	0.169	4.1	15
7	EDH	Pt-ZnO	Batch	340	0.1 (0.9 Ar)	6.4	98	6.272	0.87	16

[a]The reference numbers correspond to references in the main text.

References

(1) Sarver, P. J.; Bissonnette, N. B.; MacMillan, D. W. C. Decatungstate-Catalyzed C(Sp^3)–H Sulfinylation: Rapid Access to Diverse Organosulfur Functionality. *J. Am. Chem. Soc.* **2021**, *143* (26), 9737–9743. https://doi.org/10.1021/jacs.1c04722.

(2) Protti, S.; Ravelli, D.; Fagnoni, M.; Albini, A. Solar Light-Driven Photocatalyzed Alkylations. Chemistry on the Window Ledge. *Chem. Commun.* **2009**, No. 47, 7351–7353. https://doi.org/10.1039/B917732A.

(3) Purwanto; Deshpande, R. M.; Chaudhari, R. V.; Delmas, H. Solubility of Hydrogen, Carbon Monoxide, and 1-Octene in Various Solvents and Solvent Mixtures. *J. Chem. Eng. Data* **1996**, *41* (6), 1414–1417. https://doi.org/10.1021/je960024e.

(4) Frisch, M. J.; Trucks, G. W.; Schlegel, H. B.; Scuseria, G. E.; Robb, M. A.; Cheeseman, J. R.; Scalmani, G.; Barone, V.; Petersson, G. A.; Nakatsuji, H.; Li, X.; Caricato, M.; Marenich, A. V.; Bloino, J.; Janesko, B. G.; Gomperts, R.; Mennucci, B.; Hratchian, H. P.; Ortiz, J. V.; Izmaylov, A. F.; Sonnenberg, J. L.; Williams; Ding, F.; Lipparini, F.; Egidi, F.; Goings, J.; Peng, B.; Petrone, A.; Henderson, T.; Ranasinghe, D.; Zakrzewski, V. G.; Gao, J.; Rega, N.; Zheng, G.; Liang, W.; Hada, M.; Ehara, M.; Toyota, K.; Fukuda, R.; Hasegawa, J.; Ishida, M.; Nakajima, T.; Honda, Y.; Kitao, O.; Nakai, H.; Vreven, T.; Throssell, K.; Montgomery Jr., J. A.; Peralta, J. E.; Ogliaro, F.; Bearpark, M. J.; Heyd, J. J.; Brothers, E. N.; Kudin, K. N.; Staroverov, V. N.; Keith, T. A.; Kobayashi, R.; Normand, J.; Raghavachari, K.; Rendell, A. P.; Burant, J. C.; Iyengar, S. S.; Tomasi, J.; Cossi, M.; Millam, J. M.; Klene, M.; Adamo, C.; Cammi, R.; Ochterski, J. W.; Martin, R. L.; Morokuma, K.; Farkas, O.; Foresman, J. B.; Fox, D. J. Gaussian 16 Rev. C.01, 2016.

(5) Perdew, J. P.; Burke, K.; Ernzerhof, M. Generalized Gradient Approximation Made Simple. *Phys. Rev. Lett*. **1996**, 77, 3865–3868. ***Erratum:*** *Phys. Rev. Lett.* **1997**, 78, 1396. https://doi.org/10.1103/PhysRevLett.77.3865

(6) Adamo, C; Barone, V. Toward reliable density functional methods without adjustable parameters: The PBE0 model. *J. Chem. Phys.* **1999**, 110, 6158–6170. https://doi.org/10.1063/1.478522

(7) Weigend, F.; Ahlrichs, R. Balanced Basis Sets of Split Valence, Triple Zeta Valence and Quadruple Zeta Valence Quality for H to Rn: Design and Assessment of Accuracy. *Phys. Chem. Chem. Phys.* **2005**, *7* (18), 3297–3305. https://doi.org/10.1039/B508541A.

(8) Grimme, S.; Antony, J.; Ehrlich, S.; Krieg, H. A Consistent and Accurate Ab Initio Parametrization of Density Functional Dispersion Correction (DFT-D) for the 94 Elements H-Pu. *J. Chem. Phys.* **2010**, *132* (15), 154104. https://doi.org/10.1063/1.3382344.

(9) Grimme, S.; Ehrlich, S.; Goerigk, L. Effect of the Damping Function in Dispersion Corrected Density Functional Theory. *J. Comput. Chem.* **2011**, *32* (7), 1456–1465. https://doi.org/10.1002/jcc.21759.

(10) Luchini, G.; Alegre-Requena, J. V.; Funes-Ardoiz, I.; Paton, R. S. GoodVibes: Automated Thermochemistry for Heterogeneous Computational Chemistry Data. F1000Research April 24, 2020. https://doi.org/10.12688/f1000research.22758.1.

(11) Grimme, S. Supramolecular Binding Thermodynamics by Dispersion-Corrected Density Functional Theory. *Chem. – Eur. J.* **2012**, *18* (32), 9955–9964. https://doi.org/10.1002/chem.201200497.

(12) Waele, V. D.; Poizat, O.; Fagnoni, M.; Bagno, A.; Ravelli, D. Unraveling the Key Features of the Reactive State of Decatungstate Anion in Hydrogen Atom Transfer (HAT) Photocatalysis. *ACS Catal.* **2016**, *6* (10), 7174–7182. https://doi.org/10.1021/acscatal.6b01984.

(13) Ravelli, D.; Fagnoni, M.; Fukuyama, T.; Nishikawa, T.; Ryu, I. Site-Selective C–H Functionalization by Decatungstate Anion Photocatalysis: Synergistic Control by Polar and Steric Effects Expands the Reaction Scope. *ACS Catal.* **2018**, *8* (1), 701–713. https://doi.org/10.1021/acscatal.7b03354.

(14) Ji, X.; Ma, Y.; Sun, X.; Song, S.; Yang, K.; Huang, W.; Xu, C.; Feng, B.; Liu, J.; Song, W. Photothermal Propane Dehydrogenation Catalyzed by VO_x-Doped TiO_2 Nanoparticles. *ACS Appl. Nano Mater.* **2023**, *6* (7), 6354–6364. https://doi.org/10.1021/acsanm.3c00794.

(15) Hu, Z.; Zhu, J.; Chen, R.; Wu, Y.; Zheng, K.; Liu, C.; Pan, Y.; Chen, J.; Sun, Y.; Xie, Y. High-Rate and Selective C_2H_6-to-C_2H_4 Photodehydrogenation Enabled by Partially Oxidized $Pd^{\delta+}$ Species Anchored on ZnO Nanosheets under Mild Conditions. *J. Am. Chem. Soc.* **2024**, *146* (24), 16490–16498. https://doi.org/10.1021/jacs.4c02827.

(16) Guo, W.; Shi, W.; Cai, J.; Wei, F.; Lin, X.; Lu, X.; Ding, Z.; Hou, Y.; Zhang, G.; Wang, S. Photocatalytic Ethene Synthesis from Ethane Dehydrogenation with High Selectivity by ZnO-

Supported Pt Nanoparticles. *Catal. Sci. Technol.* **2024**, *14* (10), 2921–2928. https://doi.org/10.1039/D4CY00359D.